

MECHANICAL PROPERTIES OF NIOBIUM CAVITIES*

G. Ciovati[#], P. Dhakal, J. Matalevich, G. R. Myneni, JLab, Newport News, VA 23606, USA

Abstract

The mechanical stability of bulk Nb cavity is an important aspect to be considered in relation to cavity material, geometry and treatments. Mechanical properties of Nb are typically obtained from uniaxial tensile tests of small samples. In this contribution we report the results of measurements of the resonant frequency and local strain along the contour of single-cell cavities made of ingot and fine-grain Nb of different purity subjected to increasing uniform differential pressure, up to 6 atm. Measurements have been done on cavities subjected to different heat treatments. Good agreement between finite element analysis simulations and experimental data in the elastic regime was obtained with a single set of values of Young's modulus and Poisson's ratio. The experimental results indicate that the yield strength of medium-purity ingot Nb cavities is higher than that of fine-grain, high-purity Nb.

INTRODUCTION

An important aspect of cavity design is a structural analysis under different load conditions to verify that the maximum stress is well below the yield strength of the material. Typically, the highest load applied to the cavities occurs at the beginning of a cavity cool-down from 300 K to liquid He temperature inside a cryomodule, when loading due to a mechanical tuner attached to the cavity and pressurized helium gas flowing around the cavity occurs [1]. In recent years, it was also realized that cavities can be considered part of a "pressure vessel", as they are part of the boundary of a liquid helium reservoir, and therefore the structural and material analysis should comply with "pressure vessel code" specifications, which are different in different regions of the world [2-4].

The structural analysis of cavities is typically done using commercial finite-element analysis (FEA) computer software, with user-defined stress versus strain curves for the niobium material. Such stress versus strain curves are derived from "conservative" reviews of literature data from uniaxial tensile tests of flat samples which had been subjected to different treatments. The literature data show a progressive reduction of both yield and tensile strength of fine-grain (ASTM ≥ 5) Nb after heat-treatment at increasingly higher temperature, above ~ 600 °C [5-7]. Large variations in the values of yield and tensile strength have been reported even for samples subjected to the same treatment, depending on batches of material and/or

material supplier [8-11]. The situation is even more complicated when considering ingot Nb material, for which tensile test samples only have a very small number of grains, if any, which results in a large variability in tensile test results, depending on the crystal orientation of the samples [7, 12-14]. Furthermore, the Nb material is subjected to a plastic deformation during the deep-drawing into half-cells and, as a result of the subsequent annealing of the entire Nb cavity, the behaviour of the material under mechanical loading can, in general, be different than for the case of flat tensile test samples which have no initial plastic deformation [15].

In the following section we present some results on the measurements of the local strain and resonant frequency of single-cell elliptical Nb cavities of the same shape subjected to an increasing uniform external pressure at room temperature. The experimental data have been used to guide the FEA of the cavity.

EXPERIMENTAL RESULTS

The single-cell cavities used for this study have the same shape as that of the original cavities for the CEBAF accelerator [16]. A schematic drawing of the cavity is shown in Fig. 1 along with a schematic of the location of the strain gages. The strain gages attached near the iris are "tee rosettes", allowing to measure strain in the longitudinal (gages No. 1 and 3) and azimuthal directions (gages No. 2 and 4). The strain gages attached on the side wall (gage No. 5) and close to the equator (gage No. 6) measured strain in the longitudinal direction. Further details about the strain gages and the experimental setup can be found in Ref. [17] and in a forthcoming publication.

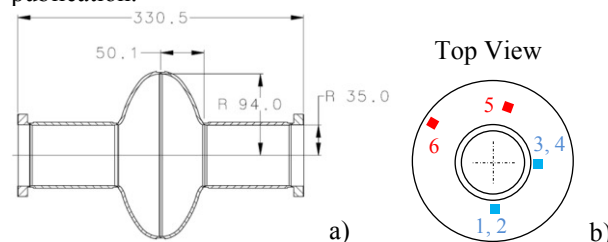


Figure 1: Schematic drawing of the single-cell cavity (a) and approximate location of the strain gages (b). Dimensions are in mm.

Cavities were placed inside a pressure tank. The inside volume of the cavity was filled with air at 1 atm. Uniform pressure is applied to the outside surface of the cavity by pumping DI water into the pressure tank. Strain, $\Delta\epsilon$, and frequency shift, Δf , as a function of applied pressure, P , were measured on four single-cell cavities made of Nb material with different properties, listed in Table 1. The fine-grain material was from ATI Wah Chang, the ingot

* This manuscript has been authored by Jefferson Science Associates, LLC under U.S. DOE Contract No. DE-AC05-06OR23177. The U.S. Government retains a non-exclusive, paid-up, irrevocable, world-wide license to publish or reproduce this manuscript for U.S. Government purposes.

[#]gciovati@jlab.org

material was from CBMM. The average wall thickness was measured for each cavity prior to the pressure test and ranged between 2.8-3.0 mm. The range of residual resistivity ratio (RRR) for each ingot results from measurements of thermal conductivity and electrical resistivity of different samples.

Table 1: Material Properties of the Cavities Used for the Pressure Tests

Cavity label	Material type	RRR	Ta content (wt.ppm)
FG	Fine-grain	>250	<500
F3F4	Ingot F	100-160	1330
G1G2	Ingot G	100-160	1375
H1H2	Ingot H	100-200	704

The series of treatments for each cavity prior to the pressure tests are as follows:

- FG: ~140 μm etching by buffered chemical polishing (BCP), ~30 μm vertical electropolishing (EP), annealing at 600 $^{\circ}\text{C}/10$ h, ~130 μm removal by centrifugal barrel polishing (CBP), 600 $^{\circ}\text{C}/10$ h heat treatment, ~7 μm horizontal EP. After the first pressure test the cavity was annealed at 800 $^{\circ}\text{C}/2$ h and the pressure test was repeated.
- F3F4: the first pressure test was just after fabrication, without any treatment. After the test, ~100 μm CBP followed by ~50 μm BCP and annealing at 800 $^{\circ}\text{C}/2$ h were applied, after which the pressure test was repeated.
- G1G2: ~70 μm CBP, ~65 μm BCP, annealing at 800 $^{\circ}\text{C}/3$ h, 800 $^{\circ}\text{C}/6$ h, 1000 $^{\circ}\text{C}/6$ h, 1200 $^{\circ}\text{C}/6$ h, 1400 $^{\circ}\text{C}/3$ h, 1400 $^{\circ}\text{C}/3$ h for a second time, 1400 $^{\circ}\text{C}/3$ h for a third time, 1250 $^{\circ}\text{C}/3$ h, 1300 $^{\circ}\text{C}/3$ h. About 10-30 μm were etched by BCP after each heat treatment. The final treatments prior to the pressure test was a heat treatment at 800 $^{\circ}\text{C}/3$ h with a nitrogen pressure ~2.7 Pa held inside the vacuum furnace for 2 min before furnace cool-down followed by ~7 μm removal by horizontal EP.
- H1H2: ~70 μm BCP, annealing at 600 $^{\circ}\text{C}/10$ h and 1400 $^{\circ}\text{C}/3$ h, ~30 μm CBP, ~50 μm BCP, ~20 μm horizontal EP. The final treatment prior to pressure test was a heat treatment at 1400 $^{\circ}\text{C}/30$ min.

3D models of the cavities for FEA were created from CMM measurements of the outer contour of one of the cavities, with thickness equal to the average thickness of each cavity. The FEA was done with ANSYS Workbench 14.5, where an elastic static structural model was considered and the niobium material properties were defined as isotropic. The peak von Mises stress, σ_v , is located near the iris of the cavity. The pressure sensitivity calculation was done as a combined structural and electromagnetic analysis. Figure 2 shows the measured $\Delta f(P)$ for all cavities along with the result from FEA with

a fixed value of Young's modulus, E , Poisson's ratio, ν and thickness, d . The measured values of $\Delta f(P)$ are between -0.68 Hz/Pa and -0.75 Hz/Pa, for cavities with $d = 3$ mm and $d = 2.8$ mm, respectively. The $\Delta f(P)$ from FEA with $E = 88.5$ GPa and $\nu = 0.4$ are within 7% of the measured values.

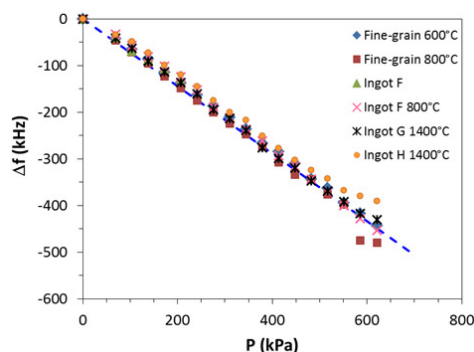


Figure 2: $\Delta f(P)$ measured for the single-cell cavities after different heat treatments. The solid line is the result from FEA with $E = 88.5$ GPa, $\nu = 0.4$, $d = 2.8$ mm.

An example of the local strain measured at the iris and equator for the single-cell F3F4 after fabrication is shown in Fig. 3, along with results from FEA.

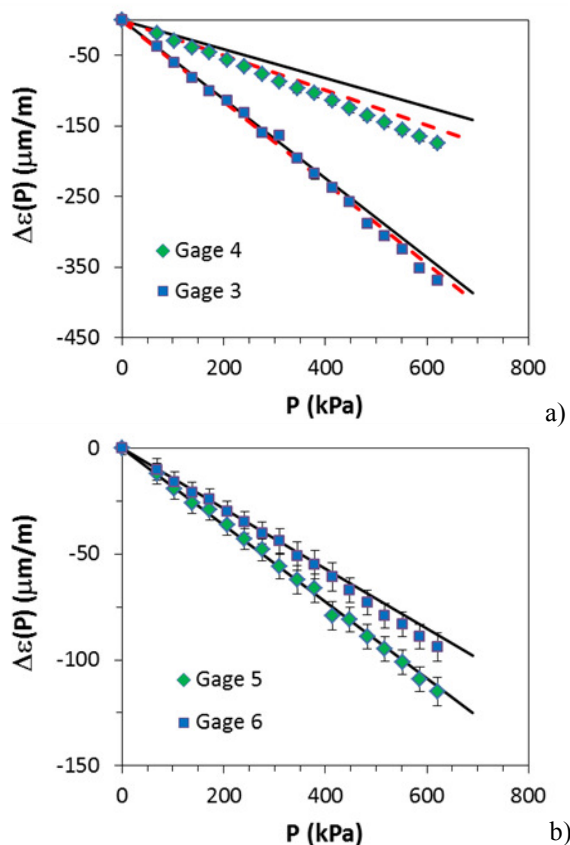


Figure 3: $\Delta \epsilon(P)$ measured at the iris (a) and equator (b) regions of ingot Nb single-cell cavity F3F4 after fabrication. Solid and dashed lines are results from FEA with $E = 88.5$ GPa, $\nu = 0.4$ and $\nu = 0.35$, respectively.

Content from this work may be used under the terms of the CC BY 3.0 licence (© 2015). Any distribution of this work must maintain attribution to the author(s), title of the work, publisher, and DOI.

Measurements of strain and frequency after relieving the pressure back to 1 atm, following each pressurization step, can be used to determine when plastic deformation occurred, as it would result in a systematic deviation of $\epsilon(0)$ and $f(0)$ from constant values. Figure 4 shows an example of $\epsilon(0)$ and $f(0)$, measured after relieving the pressure P applied to the FG cavity after 800 °C/2 h annealing. Plastic deformation at the iris (gages 1-4) result in stretching of the material in the azimuthal direction (gages 2 and 4) and compression in the longitudinal direction (gages 1 and 3). Plastic deformation closer to the equator (gages 5 and 6) occurs at higher applied pressure than at the iris, as expected from FEA. A “macro-yield” pressure of the cavity was determined from the point of intersection between linear fits of $f(0)$ vs. P below 200 kPa and above 500 kPa. A summary of the yield pressure, P_y , of the peak von Mises stress at yield pressure from FEA, $\sigma_{v,y}$, and of the yield strength values from literature, σ_y , is given in Table 2 for all cavities along with the highest annealing temperature.

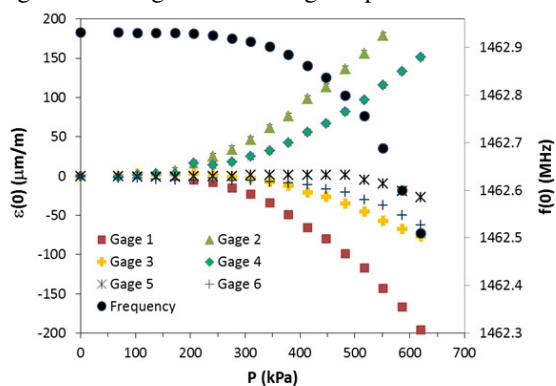


Figure 4: Strain in the iris (gages 1-4) and equator (gages 5 and 6) regions and resonant frequency measured after relieving a uniform pressure applied to the fine-grain cavity FG after 800 °C/2 h heat treatment.

Table 2: Summary of macro-yield pressure of the different cavities, for different annealing temperatures, and comparison with literature values of yield-strength.

Cavity label	Highest annealing T (°C)	P_y (kPa)	$\sigma_{v,y}$ (kPa)	σ_y (kPa)
FG	600	>620 ¹	>52	48-72 [4]
FG	800	459	39	38-45 [4]
F3F4	-	>620	>46	30-40 [14]
F3F4	800	>620	>48	n/a
G1G2	1400	517	40	56 [18]
H1H2	1400	503	40	56 [18]

¹The data show evidence of “micro-yielding” [6].

CONCLUSIONS

The results from the pressure tests and finite-element analysis of Nb single-cell cavities described in the previous sections lead to the following conclusions:

- The yield strength of fine-grain Nb is reduced by high-temperature annealing. This effect is well known from sample studies and it is related to grain-growth during annealing. In the case of high-purity (RRR>300) Nb, a reduction in yield strength is observed already after annealing at 800 °C/2 h.
- The purity of the Nb has a bigger influence on the yield strength than the grain size. Ingot Nb cavities of medium-purity showed a higher yield strength than high-purity fine-grain ones, for the same annealing temperature. Annealing medium purity, ingot Nb cavities at 1400 °C resulted in a yield pressure comparable to that of a high-purity, fine-grain Nb cavity annealed at 800 °C
- Material parameters which resulted in a good agreement between FEA and experiments, regarding the macroscopic elastic behaviour of both medium-purity, ingot Nb and high-purity fine-grain Nb cavities were $E = 88.5$ GPa and $\nu = 0.4$. Values of E and ν typically found in the literature are between 105-124 GPa and 0.27-0.4 [19, 20-23], respectively.

ACKNOWLEDGEMENTS

We would like to acknowledge B. Carpenter and J. Henry for help with the 3D model of the cavities, J. Mammosser and S. Yang for procuring the pressure tank, S. Dutton for help with the wiring of the strain gages, J. Spradlin for the RRR measurements and P. Kneisel for helpful discussions.

REFERENCES

- [1] G. Cheng, M. Wiseman, Jefferson Lab Technical Note, TN-10-001, 2010.
- [2] T. Peterson et al., AIP Conf. Proc. 1218, 839 (2010).
- [3] C. Astefanos et al., “Design and Analysis of SRF Cavities for Pressure Vessel Code Compliance”, PAC’11, New York, March 2011, p. 1322 (2011); <http://www.JACoW.org>
- [4] G. Cheng, E. F. Daly, Jefferson Lab Technical Note, TN-09-002, 2009.
- [5] G. R. Myneni, H. Umezawa, *Materiaux & Techniques*, 7-8-9, 19 (2003).
- [6] G. R. Myneni, P. Kneisel, Jefferson Lab Technical Note, TN-02-01, 2002.
- [7] G. R. Myneni, AIP Conf. Proc. 927, 41 (2007).
- [8] P. Kneisel, G. R. Myneni, Jefferson Lab Technical Note, TN-88-097, 1988.
- [9] P. Kneisel, J. Mammosser, M. G. Rao, K. Saito, *Electron Beam Melting and Refining State of the Art*, (Bakish Materials Corporation: Englewood, 1990), 177.
- [10] G. R. Myneni, P. Kneisel, “Thermal and Mechanical Properties of Electron Beam Welded and Heat-

- Treated Niobium for TESLA”, SRF’93, Newport News, October 1993, 643 (1993); <http://www.JACoW.org>
- [11] L. D. Cooley, Proc. 7th SRF Materials Workshop, Newport News, VA, USA, 2012; <https://www.jlab.org/indico/conferenceDisplay.py?confId=20>
- [12] T. Gnäupel-Herold, G. R. Myneni, R. E. Ricker, AIP Conf. Proc. 927, 48 (2007).
- [13] A. Ermakov et al., J. of Physics: Conference Series 97, 012014 (2008).
- [14] T. R. Bieler et al., Phys. Rev. ST Accel. Beams 13, 031002 (2010).
- [15] G. Wu et al., AIP Conf. Proc. 1218, 857 (2010).
- [16] P. Kneisel, K. Nakajima, J. Kirchgessner, J. Mioduszewski, IEEE Trans. Nucl. Sci. 30(4), 3348 (1983).
- [17] G. Ciovati et al., “Mechanical Properties of Ingot Nb Cavities”, IPAC’14, Dresden, June 2014, p. 2654 (2014); <http://www.JACoW.org>
- [18] P. Dhakal et al., Phys. Rev. ST Accel. Beams 16, 042001 (2013).
- [19] G. R. Myneni, S. R. Agnew, AIP Conf. Proc. 671, 227 (2003).
- [20] A. Butch, *Pure Metals Properties: A Scientific-Technical Handbook*, (ASM Intern., Materials Park, OH, 1999), 155.
- [21] J. R. Davis (ed.), *Tensile Testing*, (ASM Intern., Materials Park, OH, 2004), 98.
- [22] R. T. Webster, *Refractory Metals and Their Industrial Applications*, R. E. Smallwood (ed.), ASTM STP 849, 20 (1984).
- [23] M. Mukhopadhyay, *Fundamental of Cryogenic Engineering*, (PHI Learning, New Delhi, 2010).